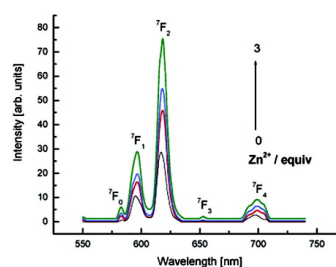
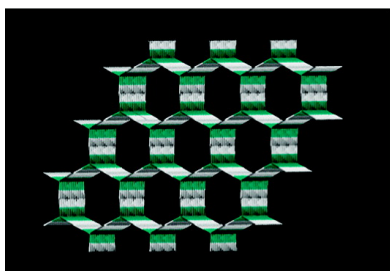


Coordination Polymers Containing 1D Channels as Selective Luminescent Probes

Bin Zhao, Xiao-Yan Chen, Peng Cheng, Dai-Zheng Liao, Shi-Ping Yan, and Zong-Hui Jiang

J. Am. Chem. Soc., **2004**, 126 (47), 15394-15395 • DOI: 10.1021/ja047141b • Publication Date (Web): 04 November 2004

Downloaded from <http://pubs.acs.org> on April 5, 2009



More About This Article

Additional resources and features associated with this article are available within the HTML version:

- Supporting Information
- Links to the 42 articles that cite this article, as of the time of this article download
- Access to high resolution figures
- Links to articles and content related to this article
- Copyright permission to reproduce figures and/or text from this article

[View the Full Text HTML](#)



ACS Publications
 High quality. High impact.

Coordination Polymers Containing 1D Channels as Selective Luminescent Probes

Bin Zhao, Xiao-Yan Chen, Peng Cheng,* Dai-Zheng Liao, Shi-Ping Yan, and Zong-Hui Jiang

Department of Chemistry, Nankai University, Tianjin 300071, P. R. China

Received May 15, 2004; E-mail: pcheng@nankai.edu.cn

The intense interest in the photophysical properties of lanthanide ion complexes has been stimulated strongly since Lehn¹ proposed that such complexes could be considered as light conversion molecular devices (LCMDs), creating the term “antenna effect” to denote the absorption, energy-transfer, emission sequence involving distinct absorbing (the ligand) and emitting (the lanthanide ion) components, thus overcoming the very small absorption coefficients of the lanthanide ions. The rapid development may result from the wide applications of efficient LCMDs in many areas, such as luminescent probes in biomedical assays and time-resolved microscopy, fluorescent lighting, luminescent sensors for chemical species (H^+ , O_2 , halide ions, OH^-), and so on.² Furthermore, several successful fluorescent chemosensors have been employed to determine the concentration of species such as H^+ , Ca^{2+} , Zn^{2+} , and Cl^- .³ Therefore, the design of efficient lanthanide complexes has become an important goal in recent years, and many intriguing complexes were reported.⁴ However, most of them contain only lanthanide metals rather than d–f mixed ones and display discrete molecules rather than multidimensional porous polymers. To our knowledge, there has been no report thus far of any investigations of the luminescent properties of d–f mixed metal-based coordination polymers, although a few examples of 3D coordination polymers based on 3d–4f mixed metals have been reported.⁵

Much experience was accumulated in designing and synthesizing d–f metal-based 3D polymers in our group.^{5a,b} As a continuation, taken into account the intriguing luminescent properties of Eu^{3+} and Tb^{3+} , two 3d–4f heterometallic coordination polymers $\{[\text{Ln}(\text{PDA})_3\text{Mn}_{1.5}(\text{H}_2\text{O})_3] \cdot 3.25\text{H}_2\text{O}\}_\infty$ with 1D channels were further synthesized under hydrothermal conditions (PDA = pyridine-2,6-dicarboxylic acid; Ln = Eu (**1**); Ln = Tb (**2**)). They exhibit high symmetry of C_6 and high thermal stabilities. Importantly, the investigations on their luminescent properties in DMF solvent show that the emission intensity of complexes **1** and **2** increased significantly upon addition of Zn^{2+} , while the introduction of other metal ions caused the intensity to be either unchanged or weakened. The case implies that **1** and **2** could monitor or recognize Zn^{2+} to some extent and be considered as luminescent probes.

Complexes **1** and **2** are isomorphous. The structural analyses⁶ revealed that they were fabricated from two types of building blocks, $\text{Ln}(\text{PDA})_3$ and $\text{MnO}_4(\text{H}_2\text{O})_2$ (see Supporting Information). Each Ln^{3+} chelated to three PDA anions as tridentate (ONO) ligand: six O atoms and three N atoms completed the nine-coordinated environment of Ln^{3+} . The octahedral geometry of Mn^{2+} was formed by four carboxyl O atoms and two water molecules. Each PDA anion chelated to Ln^{3+} combined with two Mn^{2+} by carboxyl O bridges, thus six Mn^{2+} as the nearest neighbors exist around each Ln^{3+} , while each Mn^{2+} has four Ln^{3+} in its vicinity. The adjacent Ln and Mn atoms were connected by carboxyl bridges, and most importantly, each carboxyl group also bridges a Mn–OCO–Ln unit, which is assembled into a highly ordered 3D structure with 1D channels of about 1.8-nm diameter (Figure 1). The section of the

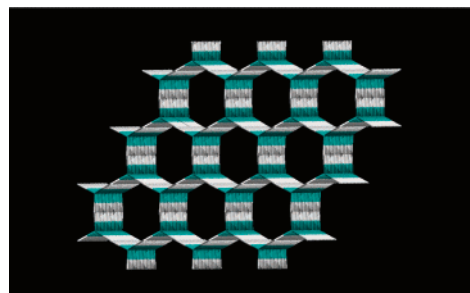


Figure 1. Backbone of the 3D nanoporous in **1**. The lines between Eu and Mn atoms stand for carboxyl bridges. Eu: cyan; Mn: gray.

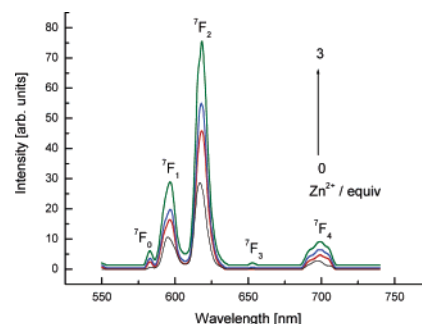


Figure 2. Emission spectra of **1** in DMF (10^{-3} M) at room temperature (excited at 287 nm) in the presence of ~0–3 equiv of Zn^{2+} ions with respect to **1**, respectively: black, no addition; red, 1 equiv; blue, 2 equiv; green, 3 equiv.

channel displays a dodecanuclear heterometallic macrocycle of $\text{Ln}_6\text{Mn}_6\text{C}_{12}\text{O}_{24}$ with C_6 symmetry, in which Ln and Mn atoms connected via O–C–O bridges are arrayed alternately.

The magnetic susceptibility measurements of **1** show that, with decreasing temperature, the $\chi_{\text{M}}T$ value of **1** decreases gradually and then drops rapidly in the lower temperature region (see Supporting Information). Although the $\chi_{\text{M}}T$ value for **1** smoothly decreases on cooling, the nature of the magnetic coupling between adjacent Eu and Mn ions could not be interpreted as antiferromagnetic interaction due to the existence of strong spin–orbit coupling for lanthanide atoms.⁷ While the $\chi_{\text{M}}T$ value of **2** slowly increases on cooling and reaches a maximum of $18.81 \text{ cm}^3 \text{ K mol}^{-1}$ at 110 K, this behavior indicates ferromagnetic coupling between Tb^{3+} and Mn^{2+} , which is observed for the first time in Ln–Mn systems. Then the $\chi_{\text{M}}T$ value dramatically drops on further cooling owing to the decrease of the $\chi_{\text{M}}^{\text{Tb}}T$ value for Tb^{3+} itself, which further confirms that the ferromagnetic coupling between Tb^{3+} and Mn^{2+} is predominant above 110 K.⁸

The emission spectrum of **1** (Figure 2) at room temperature in DMF solution excited at 287 nm exhibits the characteristic transition of the Eu^{3+} ion: $^5\text{D}_0 \rightarrow ^7\text{F}_J$ ($J = 0, 1, 2, 3, 4$). The symmetric forbidden emission $^5\text{D}_0 \rightarrow ^7\text{F}_0$ at 580 nm can be found in **1**. It is well-known that the $^5\text{D}_0 \rightarrow ^7\text{F}_0$ transition is strictly forbidden in a

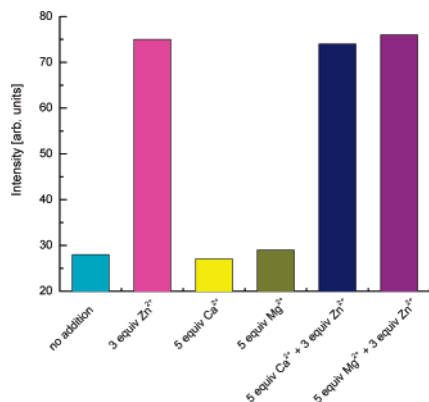


Figure 3. Luminescent intensity of complex **1** at 618 nm in DMF at room temperature upon the addition of Zn²⁺, Ca²⁺, or Mg²⁺ ions (excited at 287 nm). Cations were added as ZnCl₂, CaCl₂, or MgCl₂.

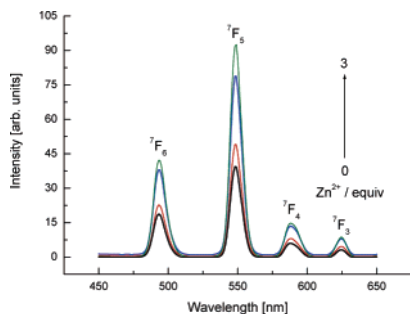


Figure 4. Emission spectra of **2** in DMF (10⁻³ M) at room temperature (excited at 296 nm) in the presence of ~0–3 equiv of Zn²⁺ ions with respect to **2**, respectively: black, no addition; red, 1 equiv; blue, 2 equiv; green, 3 equiv.

field of symmetry. Thus, the above result reveals that Eu³⁺ in **1** occupies sites with low symmetry and without an inversion center.⁹ Interestingly, the emission intensity of **1** increased gradually upon addition of 1–3 equiv of Zn²⁺ with respect to **1**. The highest peak at 618 nm is at least twice as intense as the corresponding band in the solution without Zn²⁺. To make a further understanding of this phenomenon, the same experiments were performed for the introduction of Ca²⁺ and Mg²⁺ into the system. Even the presence of 5 equiv of Ca²⁺ or Mg²⁺ in DMF solution of **1** has no effect on the luminescent intensities either (Figure 3). While adding 1–3 equiv of Mn²⁺ to the solution of **1**, the luminescent intensities decreased. Other transition metals such as Fe²⁺, Co²⁺, and Ni²⁺ quenched the luminescence of **1**.

The luminescent spectrum of **2** (Figure 4) exhibits the characteristic transition of Tb³⁺. The sharp lines are assigned to transition between the first excited state ⁵D₄ and the ground multiplet ⁷F_{6–3} for Tb³⁺,¹⁰ respectively. Although the lanthanide ions in **1** and **2** are different, the luminescent intensities of **2** changed in an extremely similar way to that of **2** when transition metals were added, namely, the introduction of Zn²⁺ increased the luminescent intensities of **2**, and with the enhancement of Zn²⁺ concentration, the luminescent intensities enhanced accordingly. While the introduction of other metal ions such as Mn²⁺, Ca²⁺, Mg²⁺, Fe²⁺, Co²⁺, and Ni²⁺ would cause the luminescent intensities of **2** to be either unchanged or weakened even if quenched (see Supporting Information).

It is well-known that the luminescent intensity of the Ln³⁺ relies on the efficiency of the energy transfer from the ligand to Ln³⁺

center.^{10a} According to the above results, the energy transfer process is more effective with the addition of certain transition metal ions.^{11,12} The reported Zn²⁺-sensitive luminescent lanthanide probe operates through a photoinduced electron-transfer process.¹³ In this contribution, the enhancement of luminescent intensity may result from more effective intramolecular energy transfer from the PDA ligand to the Ln³⁺.

As luminescent probes, the 3D coordination network possesses high thermal stability, which is confirmed by thermal gravimetric analysis (TGA) on crystalline samples of these compounds in the range from 18 to 595 °C. The TGA and EA results reveal that one water molecule was absorbed per EuMn_{1.5} and TbMn_{1.5} unit, respectively, due to the large channels existing in the polymers. Both complexes did not decompose until 400 °C (see Supporting Information).

In summary, two luminescent 3D polymers with d–f mixed metals were synthesized by hydrothermal methods, which is the first example of the combination of unique luminescent properties and intriguing nanoporous coordination polymers based on d–f metals. Most importantly, the luminescence of both **1** and **2** displayed high-performance selectivity for Zn²⁺, which implies that they may be used as luminescent probes of Zn²⁺. These results provide an opening into a promising new field of luminescent probes based on nanoporous d–f heterometallic coordination polymers.

Acknowledgment. This work was supported by the NSFC (Nos. 90101028, 50173011) and the TRAPOYT of MOE, China.

Supporting Information Available: Complete experimental procedures and characterization data (PDF and CIF) and plots. This material is available free of charge via the Internet at <http://pubs.acs.org>.

References

- Lehn, J. M. *Angew. Chem., Int. Ed. Engl.* **1990**, *29*, 1304–1319.
- (a) Sabbatini, N.; Guardigli, M.; Lehn, J. M. *Coord. Chem. Rev.* **1993**, *123*, 201–228. (b) Mikola, H.; Takkalo, H.; Hemmilä, I. *Bioconj. Chem.* **1995**, *6*, 235–241. (c) Parker, D.; Kanthi-Senanayake, P.; Williams, J. A. G. *J. Chem. Soc., Perkin Trans.* **1998**, *2*, 2129–2139.
- Lowe, M. P.; Parker, D. *Chem. Commun.* **2000**, 707–708.
- (a) Liu, W. S.; Jiao, T. Q.; Li, Y. Z.; Liu, Q. Z.; Tan, M. Y.; Wang, H.; Wang, L. F. *J. Am. Chem. Soc.* **2004**, *126*, 2280–2281. (b) Glover, P. B.; Ashton, P. R.; Childs, L. J.; Rodger, A.; Kercher, M.; Williams, R. M.; Cola, L.; Pikramenou, Z. *J. Am. Chem. Soc.* **2003**, *125*, 9918–9919. (c) Gunnlaugsson, T.; Leonard, J. P.; Senechal, K.; Harte, A. J. *J. Am. Chem. Soc.* **2003**, *125*, 12062–12063. (d) Fabbri, L.; Licchelli, L.; Pallavicini, P. *Acc. Chem. Res.* **1999**, *32*, 846–853.
- (a) Zhao, B.; Cheng, P.; Dai, Y.; Cheng, C.; Liao, D. Z.; Yan, S. P.; Jiang, Z. H.; Wang, G. L. *Angew. Chem., Int. Ed.* **2003**, *42*, 934–936. (b) Zhao, B.; Cheng, P.; Chen, X. Y.; Cheng, C.; Shi, W.; Liao, D. Z.; Yan, S. P.; Jiang, Z. H. *J. Am. Chem. Soc.* **2004**, *126*, 3012–3013. (c) Baggio, R.; Garland, M. T.; Moreno, Y.; Peña, O.; Perec, M.; Spodine, E. *J. Chem. Soc., Dalton Trans.* **2000**, 2061–2066.
- Crystal data for **1**, *M*_r = 842.28, hexagonal, *P6/mcc*, *a* = 15.288(3), *b* = 15.288(3), *c* = 15.663(6) Å, γ = 120°, *Z* = 4, *R*₁ = 0.0283 (*I* > 2σ(*I*)). *GOF* = 0.997. Crystal data for **2**, *M*_r = 849.24, hexagonal, *P6/mcc*, *a* = 15.351(4), *b* = 15.351(4), *c* = 15.812(8) Å, γ = 120°, *Z* = 4, *R*₁ = 0.0341 (*I* > 2σ(*I*)). *GOF* = 1.146.
- Benelli, C.; Gatteschi, D. *Chem. Rev.* **2002**, *102*, 2369–2387.
- Kahn, M. L.; Sutter, J.-P.; Golhen, S.; Guionneau, P.; Ouahab, L.; Kahn, O.; Chasseau, D. *J. Am. Chem. Soc.* **2000**, *122*, 3413–3421.
- (a) Nogami, M.; Abe, Y. *J. Non-Cryst. Solids* **1996**, *197*, 73–78. (b) Xu, Q. H.; Li, L. S.; Liu, X. S.; Xu, R. R. *Chem. Mater.* **2002**, *14*, 549–555.
- (a) Arnaud, N.; Vaquer, E.; Georges, J. *Analyst* **1998**, *123*, 261–265. (b) Reineke, T. M.; Eddaoudi, M.; Fehr, M.; Kelley, D.; Yaghi, O. M. *J. Am. Chem. Soc.* **1999**, *121*, 1651–1657.
- Hanaoka, K.; Kikuchi, K.; Kojima, H.; Urano, Y.; Nagano, T. *Angew. Chem., Int. Ed.* **2003**, *42*, 2996–2999.
- (a) Sá, de C. F.; Malta, O. L.; Mello Donegá, de C. A.; Simas, M.; Longo, R. L.; Santa-Cruz, P. A.; da Silva, E. F., Jr. *Coord. Chem. Rev.* **2000**, *196*, 165–195. (b) Heller, A.; Wasserman, E. *J. Chem. Phys.* **1965**, *42*, 949–955.
- Reany, D.; Gunnlaugsson, T.; Parker, D. *Chem. Commun.* **2000**, 473–474.

JA047141B